Characterising Nearby Luminous Infrared Galaxies

Rajin Ramphul[1,2]

Supervisors: Petri Vaisanen[2], Kurt van der Heyden[1]

[1]University of Cape Town, [2]South African Astronomical Observatory

1. Abstract

The classification of LIRGs, $L_{IR} > 10^{11}$ L_{sol}, and ULIRGs $L_{IR} > 10^{12}$ L_{sol} was firstly done by Sanders and Mirabel (1996) and are known to be highly interacting galaxies with strong star-formation. The cause of such high emission in the IR is due to dust enshrouded star formation, strong AGN activity or a combination of both. The dust present inside a galaxy will absorb optical/UV emission to re-emit in the infrared. Sanders and Mirabel (1996) also showed that a large fraction of the (U)LIRGs population is in mergers and a very small percentage are isolated galaxies. (U)LIRGs have therefore been proposed as an evolutionary step in the sequence between spirals and ellipticals via mergers. We present current work on a sample of nearby LIRGs, observed with the Southern African Large Telescope (SALT) in long-slit mode using RSS spectrograph. A reduction pipeline was devised for quick and efficient data reduction of the SALT/RSS data. Stellar populations modelling of the sample is done using Starlight (Cid Fernandes, 2005) which ultimately leads to understanding the star formation history of these galaxies. By subtracting the contribution of stellar continuum emission, the ionised gas emissions is measured using automatic multi-component Gaussian line fitting. This in turn is used to derive chemical abundances, star formation rates and the galaxy rotation curves to understand the galaxy kinematics.

2. Data Sample

Our sample, dubbed the SUperNovae and starBursts in the InfraReD (SUNBIRD), is part of an international survey of 40+ LIRGs and ULIRGs in a distance range of 40 to 300 Mpc, as well as a comparison sample of lower luminosity starbursts, to study in detail the physical characteristics of star formation and its triggering. The sample of galaxies is in various stages of interaction with various stages of merging, and some with strong AGN contribution. The imaging part of the survey was mainly done in the Near Infrared with VLT/NACO and also Gemini/ALTAIR/NIR making use of adaptive optics while the SALT has been used for spectroscopic follow up of the targets.

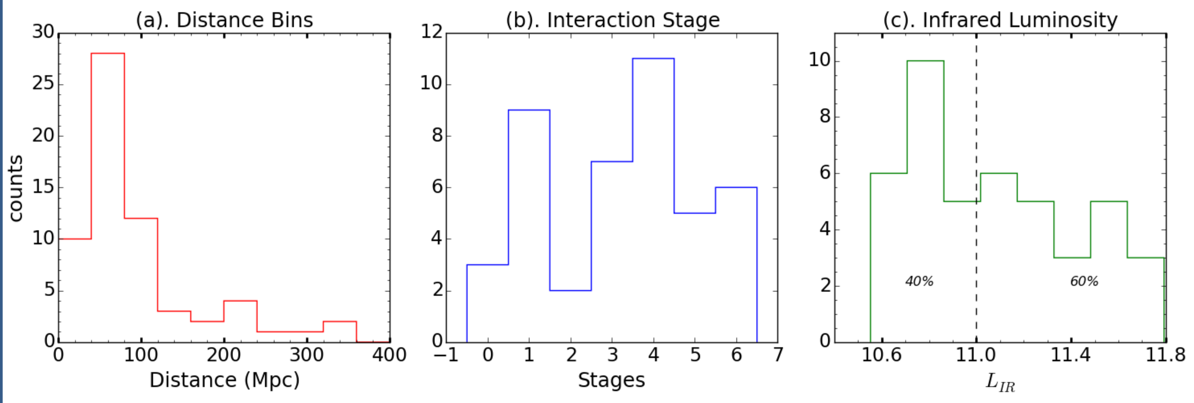

Figure 1: Some properties of our sample shown in the above histograms: (a) distances, (b) Interaction stages and (c) the IR luminosity.

3. Observations

Most targets were observed using 2 gratings: PG0900 (low resolution) and PG1800 (medium resolution), with the slit aligned along the major axis of the galaxies in most cases. PG0900 is mainly used for the stellar population work as it offers wider wavelength range coverage while ionised and neutral gas kinematics is derived from PG1800 data and chemical abundances are obtained from both. The total time on telescope was 60 hrs and some specifications is given

Grating	Range	Res	Telescope Time
PG0900	3640 - 6740 Å	0.91 Å	43 %
PG1800	5590 - 6925 Å	0.42 Å	57 %

4. Data Reduction

Due to the large amount of data collected for the project a pipeline was written to reduce spectroscopic data consistently. Error frames was propagated during the reduction process to keep the pixel by pixel variations of the noise – this is key for uncertainty estimation on recovered parameters in spectral fitting. A flow chart diagram of the procedure followed by the pipeline is shown below

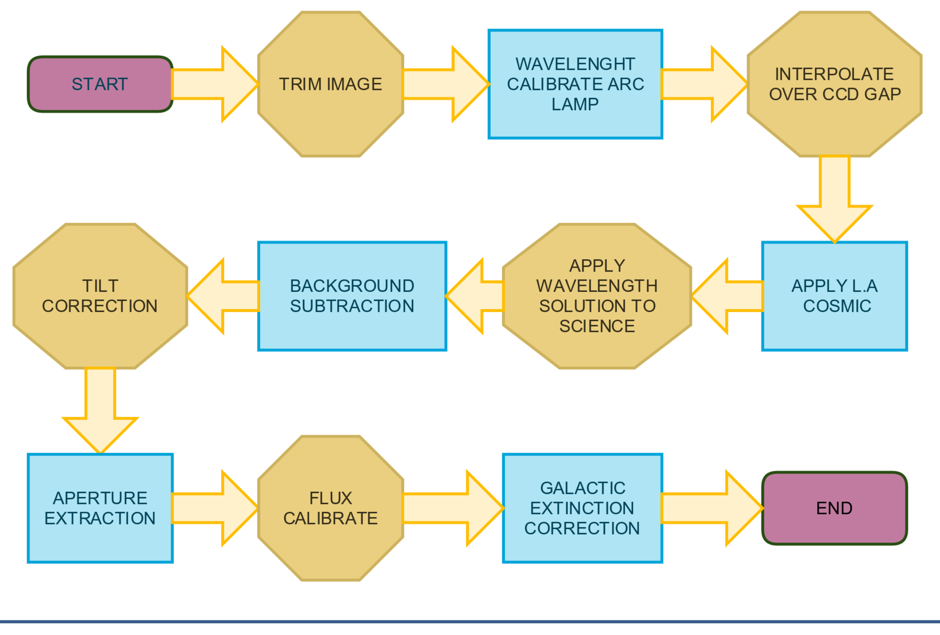

Email: rajin 250@yahoo.com

5. Stellar Population Modelling

By fitting the extracted spectra of galaxies against templates such as Bruzual & Charlot (2003), the stellar population is derived. The code Starlight is used and parameters such as age, metallicity, and extinction is recovered during the process. Noise is added on top of the spectra and several fits are done to get a distribution of results out of which the uncertainty is estimated.

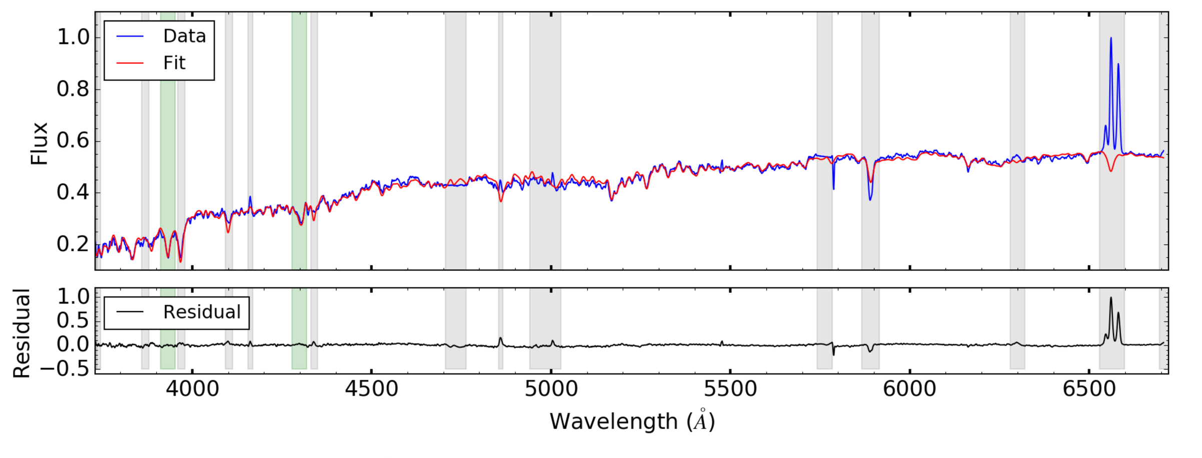

Figure 2: Fit example of ESO 154-G010. Blue line is the observed data, red is the fitted result and black is the residual after subtraction. Grey and green shaded regions are masked areas due to presence of emission lines or sky lines.

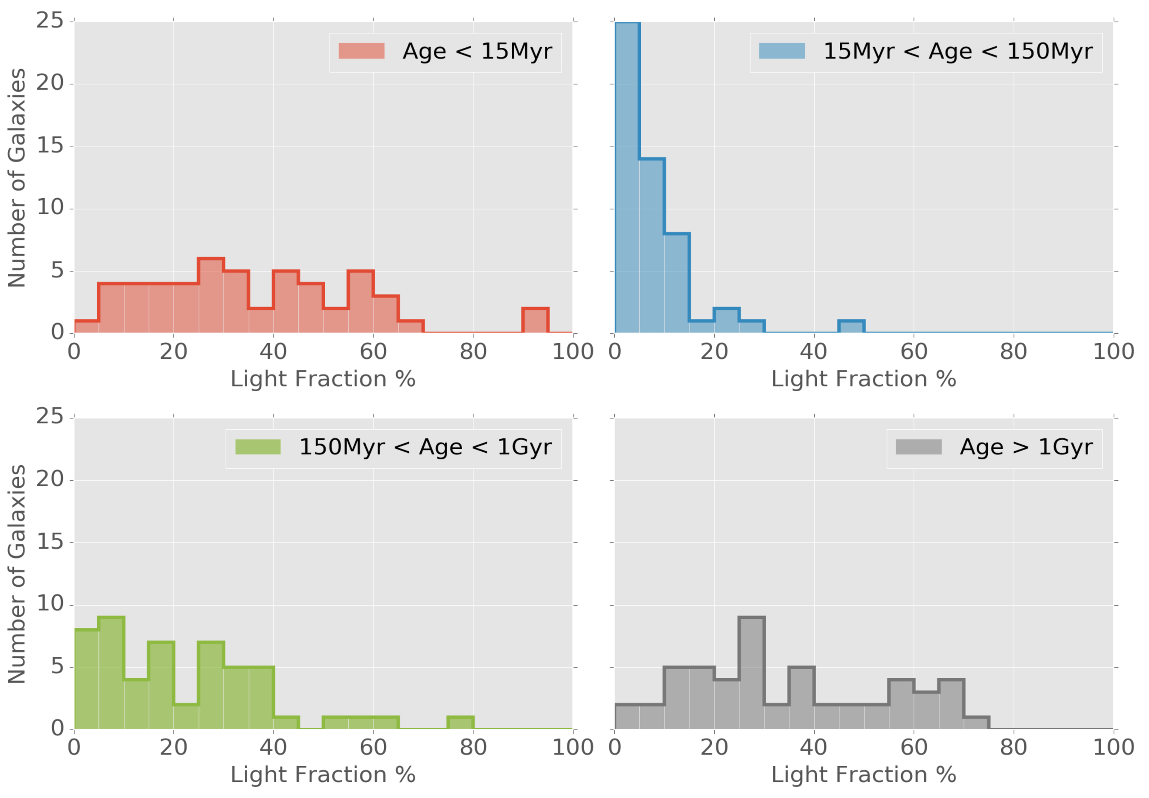

Figure 3: A breakdown of the light fraction contribution of different stellar population ages. ***We see a that the very young population is always present along with an underlying old population. Intermediate ages have a bigger variation in their contributions.***

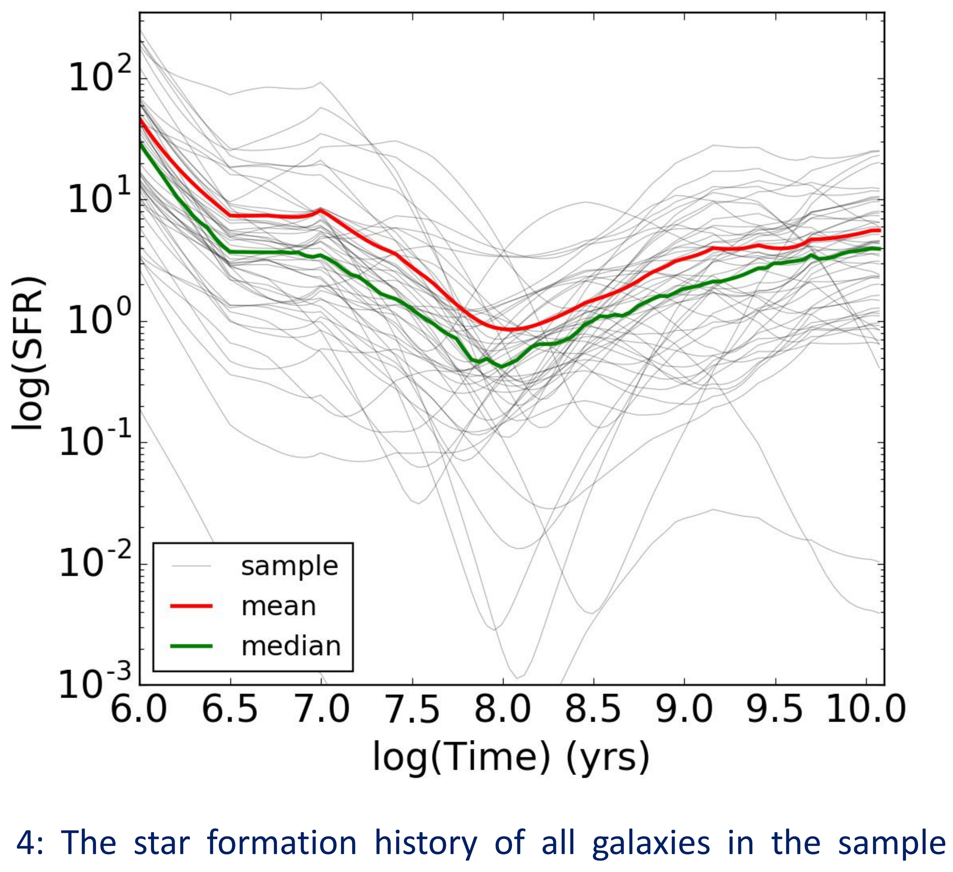

Figure 4: The star formation history of all galaxies in the sample (grey lines) with mean and median values shown in red and green respectively. From the light contribution, the time evolution of SFR is reconstructed. ***On average, after the initial burst of SF at the beginning of the universe, the galaxies go through a quiescent period before being triggered in the last ~100 Myrs when a strong burst of SF occurs***

6. $D_n(4000)$ vs $H\delta_A$

$D_n(4000)$ is an index that uses the gradient of a galaxy spectrum at 4000A-break to quantify how old its stellar population is. Similarly the $H\delta_A$ is age sensitive lick index but it has a more complex variation with age than the quasi-monotonic function of $D_n(4000)$.

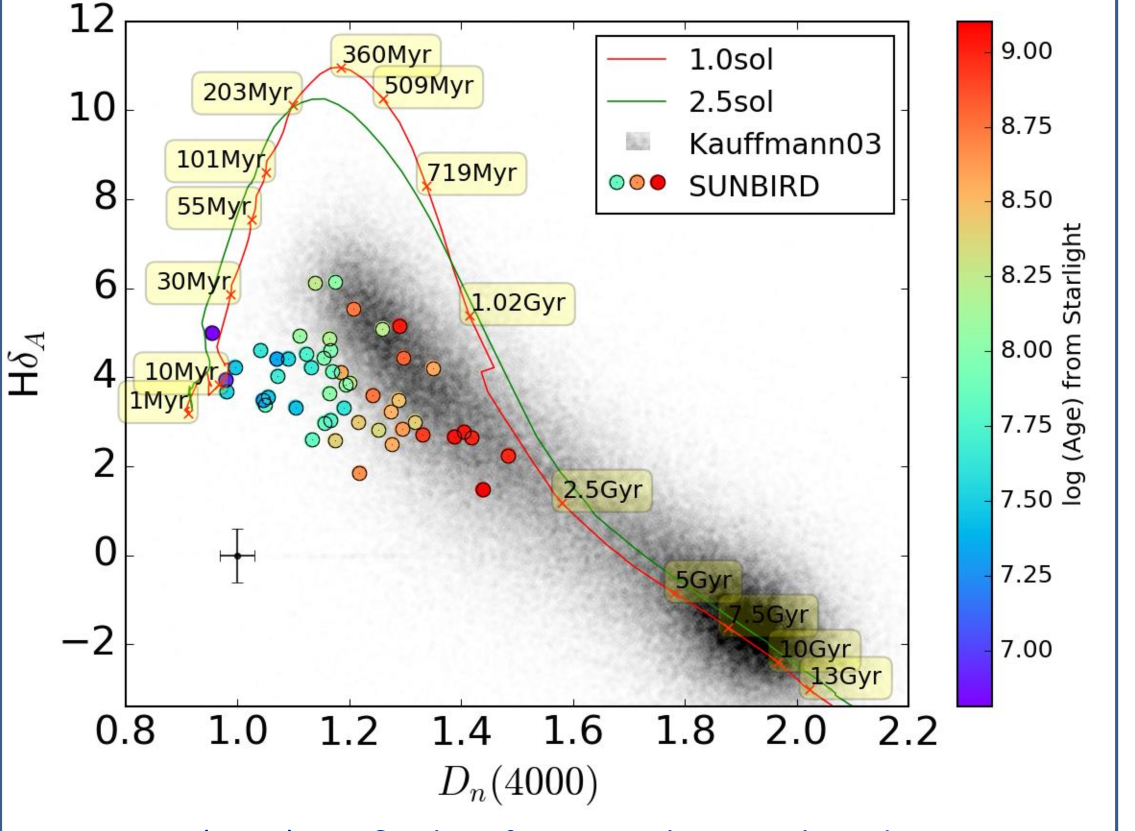

Figure 5: $D_n(4000)$ vs $H\delta_A$ plot of our sample over-plotted on top SDSS data (grey points) from Kauffmann et al. (2003). The lines (red and green) indicates the locus of the 2 indices for single burst events at different ages and 2 metallicities following BC03 models. Data points from our survey are marked by circular markers which are colour coded by the age we derived from Starlight fitting. The strong component of very young stellar population pushes most of our sample outside of the areas occupied by normal spirals and ellipticals. ***The mixture of stellar populations observed in this sample is consistent to the study made by Alonso-Herrero et al. (2009, 2010) which had a very evolved population along with a very young population***

7. Extinction

By comparing different hydrogen line ratios , the intrinsic extinction of the gas component of each object is determined. The stellar extinction on the other hand is obtained during stellar fitting.

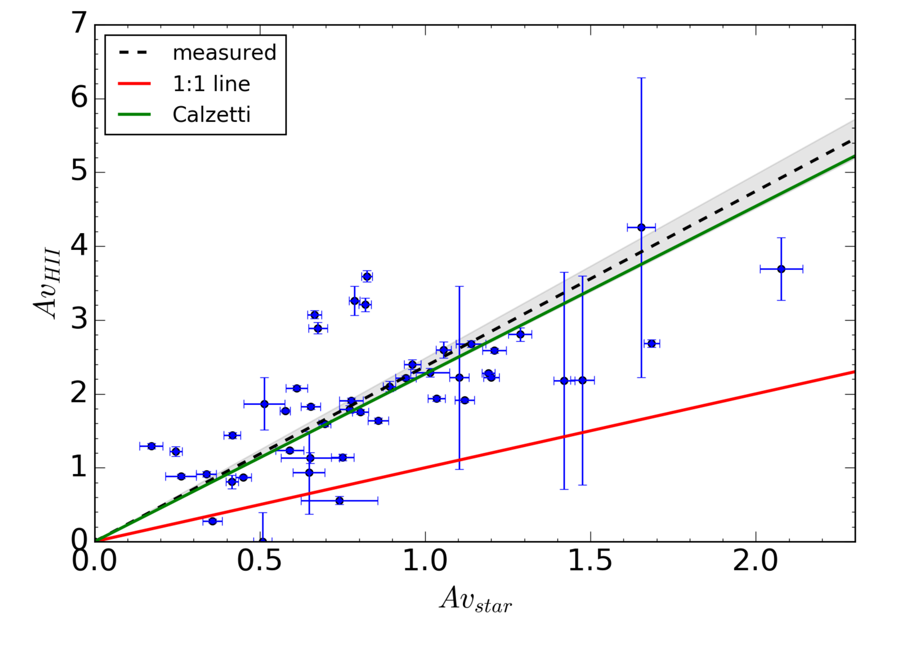

Figure 6: Stellar extinction against Ionised gas extinction comparison for each target. The red line indicates the 1:1 ratio line, while the green line is that of Calzetti (2000) and the dashed line is the measured best fit line. ***The observed ratio is consistent with a two component dust model (Calzetti (1994), Price et al. (2014)).*** This model consists of a dust component in the ISM that attenuates light from both SF regions as well as older stellar populations. The secondary component comes around the young stellar birth clouds which purely attenuates light of those regions.

8. Future work

- Derives gradient for age, metallicities, extinction from the data
- Derives the kinematics of the stellar and gas components to be able to identify gas inflows and outflows.

9. References

Sanders, D. B., Mirabel, I. F. 1996, ARAA,34, 749

Cid Fernandes, R., Mateus, A., Sodre, L., Stasínska, G., & Gomes, J. M. 2005, MNRAS, 358, 363

Bruzual, G., Charlot, S. 2003, MNRAS, 344, 1000

Kauffmann, G., Heckman, T. M., White, S. D. M., et al. 2003, MNRAS, 341, 33

Alonso-Herrero, A., Garcia-Marin, M., Monreal-Ibero, A., et al. 2009, A&A, 506, 1541

Alonso-Herrero, A., Garcia-Marin, M., Rodriguez Zaurin, J., et al. 2010, A&A, 522, A7

Calzetti, D., Armus, L., Bohlin, R. C., et al. 2000, ApJ 533, 682

Calzetti, D., Kinney, A. L., Storchi-Bergmann, T. 1994, ApJ, 429, 582

Price, S. H., Kriek, M., Brammer, G. B., et al. 2014, ApJ, 788, 86